Quantum well in a microcavity with injected squeezed vacuum

Daniel Erenso, Reeta Vyas, and Surendra Singh
Department of Physics, University of Arkansas, Fayetteville, Arkansas 72701
(Received 27 August 2002; published 31 January 2003)

A quantum well with a single exciton mode in a microcavity driven by squeezed vacuum is studied in the low exciton density regime. By solving the quantum Langevin equations, we study the intensity, spectrum, and intensity correlation function for the fluorescent light. An expression for the Q function of the field inside the cavity is derived from the solutions of the quantum Langevin equations. Using the Q function, the intracavity photon number distribution and the quadrature fluctuations for both the cavity and fluorescent fields are studied. Several interesting and new effects due to squeezed vacuum are found.

DOI: 10.1103/PhysRevA.67.013818 PACS number(s): 42.55.Sa, 78.67.De, 42.50.Dv, 42.50.Lc

I. INTRODUCTION

With the development of semiconductor optical microcavities, there has been considerable interest in exciton-cavity coupled systems [1,2]. These systems have revealed some interesting phenomena that are similar to those observed in the interaction of a two-level atom with light [3–9]. The exciton-cavity system gives rise to the so-called polaritons, which are the normal modes of a coupled exciton-photon system. The excitation spectrum of the composite exciton-cavity system is characterized by two well-resolved polariton resonances (or normal mode resonances) when $g > (\gamma_e, \gamma_c)$, where g is the dipole coupling between the exciton and the cavity mode, and γ_e and γ_c are the exciton and cavity mode damping rates, respectively. In this limit, an excitation of the cavity mode can lead to a coherent oscillatory energy exchange (or normal mode oscillation) between the exciton and the cavity due to the vacuum Rabi oscillations.

The vacuum Rabi oscillations in a coupled exciton-photon system in semiconductor microcavity lasers have been observed by Weisbuch *et al.* [2]. Following this observation, extensive experimental and theoretical studies have been carried out [10–17]. These studies have confirmed normal mode splitting and oscillatory emission from exciton microcavities. Theoretical investigations in the linear regime, where the excitons can be approximated as bosons, have been carried out by Pau *et al.* [15]. Wang *et al.* [16] investigated the effects of inhomogeneous broadening of excitons on normal mode oscillations in semiconductor microcavities using the coupled oscillator model. Their results show that inhomogeneous broadening can drastically alter the coherent oscillatory energy exchange process even in regimes where normal mode splitting remains nearly unchanged.

In this paper, we study the excitonic system in a microcavity where the cavity is driven by squeezed vacuum. An outline of the system is shown in Fig. 1. A semiconductor quantum well is embedded between two Bragg reflecting mirrors. One of these mirrors acts as an input port through which light in a squeezed vacuum state is injected into the cavity. We include dissipation of both the cavity and exciton modes. In Sec. II, we derive the quantum Langevin equations for the exciton and cavity modes. We solve these equation for the case in which the damping constants are equal. These results are used in Sec. III to study the effects of initial cavity photon number as well as squeezed-vacuum photon number on the intensity, spectrum, and the second-order intensity correlation of the fluorescent light. In Sec. IV, we obtain the Q-distribution function and use it to study the intracavity photon number distribution and squeezing of the cavity mode and the fluorescent light. We summarize the principal results of the paper in Sec. V.

II. QUANTUM LANGEVIN EQUATION

We consider a semiconductor quantum well (QW) in the linear excitation regime where the density of excitons is small so that exciton-exciton interaction can be ignored. The excitons can then be approximated as a dilute boson gas [18]. In this approximation, the microscopic Hamiltonian in the interaction picture describing the exciton-cavity system is given by [17,19]

$$\hat{H}_I = \hbar\Delta\omega\hat{b}^\dagger\hat{b} + i\hbar g(\hat{a}^\dagger\hat{b} - \hat{a}\hat{b}^\dagger) + \hat{a}\hat{\Gamma}_c^\dagger + \hat{a}^\dagger\hat{\Gamma}_c + \hat{b}\hat{\Gamma}_e^\dagger + \hat{b}^\dagger\hat{\Gamma}_e . \quad (1)$$

The Hamiltonian of Eq. (1) is written in the rotating-wave approximation and in the dipole approximation. Here $\hat{a}$ and $\hat{b}$ are the annihilation operators for the cavity and exciton modes, respectively, in a frame rotating at frequency ω_c, $\hat{\Gamma}_c$ ($\hat{\Gamma}_e$) is the reservoir operator responsible for cavity field (exciton) damping, g is the coupling constant characterizing the strength of interaction between the exciton and the cavity field, and detuning $\Delta\omega = (\omega_e - \omega_c)$, where ω_e and ω_c are the frequencies of the exciton and cavity modes, respectively. Normally, the exciton and cavity modes are coupled to a continuum of thermal reservoir modes. This leads to their

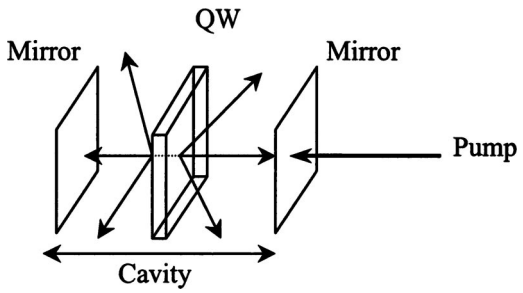

FIG. 1. An outline of the physical system.

dissipation. Here, we shall consider the case in which the cavity mode is damped by a broadband squeezed vacuum. Then the interaction Hamiltonian of Eq. (1) leads to the following quantum Langevin equations for the field and exciton operators:

$$\frac{d\hat{a}}{dt} = -\frac{\gamma_c}{2}\hat{a} + g\hat{b} + \hat{F}_c(t), \tag{2}$$

$$\frac{d\hat{b}}{dt} = -\left(\frac{\gamma_e}{2} + i\Delta\omega\right)\hat{b} - g\hat{a} + \hat{F}_e(t). \tag{3}$$

Here γ_c and γ_e are the damping rates for the cavity and exciton modes, and $\hat{F}_c$ and $\hat{F}_e$ are the noise operators for the cavity and exciton modes, respectively. Equations (2) and (3) are similar to those obtained by Pau *et al.* [15]. They solved these equations by neglecting the noise terms. In the present case, we are interested in studying the system when the cavity mode is damped by a squeezed vacuum. In this case, the noise terms are essential and must be retained. Noise operators for both the exciton and photon modes have zero mean, $\langle \hat{F}_c(t)\rangle = 0 = \langle \hat{F}_e(t)\rangle$. For the cavity mode damped by a broadband squeezed vacuum centered about the cavity mode, the noise operators have the following correlations [20]:

$$\begin{aligned}
\langle \hat{F}_c(t)\hat{F}_c^\dagger(t')\rangle &= \gamma_c(N_c+1)\,\delta(t-t'),\\
\langle \hat{F}_c^\dagger(t)\hat{F}_c(t')\rangle &= \gamma_c N_c\,\delta(t-t'),\\
\langle \hat{F}_c(t)\hat{F}_c(t')\rangle &= \gamma_c M_c\,\delta(t-t'),\\
\langle \hat{F}_c^\dagger(t)\hat{F}_c^\dagger(t')\rangle &= \gamma_c M_c^*\,\delta(t-t').
\end{aligned} \tag{4}$$

Here N_c is the mean photon number of the squeezed reservoir and M_c is a parameter related to the phase correlations of the squeezed reservoir. N_c and M_c are related to the squeezing parameter r by

$$N_c = \sinh^2(r), \quad M_c = e^{i\theta}\sinh(r)\cosh(r). \tag{5}$$

For the exciton noise operator we have

$$\begin{aligned}
\langle \hat{F}_e(t)\hat{F}_e^\dagger(t')\rangle &= \gamma_e(N_e+1)\,\delta(t-t'),\\
\langle \hat{F}_e^\dagger(t)\hat{F}_e(t')\rangle &= \gamma_e N_e\,\delta(t-t'),\\
\langle \hat{F}_e(t)\hat{F}_e(t')\rangle &= \langle \hat{F}_e^\dagger(t)\hat{F}_e^\dagger(t')\rangle = 0.
\end{aligned} \tag{6}$$

All the odd-order correlations vanish and even-order correlations can be expressed in terms of second-order correlations. N_e is the mean number of thermal phonons in the exciton bath.

To gain insight into the dynamical behavior of the system, we consider the special case when the damping rates and the frequencies of the exciton and the cavity modes are equal. Then by introducing the transformations

$$\hat{X} = \hat{a} + i\hat{b}, \quad \hat{Y} = \hat{a} - i\hat{b}, \tag{7}$$

we obtain two uncoupled equations for $\hat{X}$ and $\hat{Y}$,

$$\frac{d\hat{X}}{dt} = -\left(\frac{\gamma}{2} + ig\right)\hat{X} + [\hat{F}_c(t) + i\hat{F}_e(t)], \tag{8}$$

$$\frac{d\hat{Y}}{dt} = -\left(\frac{\gamma}{2} - ig\right)\hat{Y} + [\hat{F}_c(t) - i\hat{F}_e(t)]. \tag{9}$$

Solving these equations and using the inverse of transformation (7), we obtain the following solutions for $\hat{a}$ and $\hat{b}$:

$$\begin{aligned}
\hat{a}(t) = A_1(t)\hat{a}(0) + A_2(t)\hat{b}(0) &+ \int_0^t A_1(t-t')\hat{F}_c(t')dt'\\
&+ \int_0^t A_2(t-t')\hat{F}_e(t')dt',
\end{aligned} \tag{10}$$

$$\begin{aligned}
\hat{b}(t) = A_1(t)\hat{b}(0) - A_2(t)\hat{a}(0) &+ \int_0^t A_1(t-t')\hat{F}_e(t')dt'\\
&- \int_0^t A_2(t-t')\hat{F}_c(t')dt',
\end{aligned} \tag{11}$$

where

$$A_1(t) = e^{-\gamma t/2}\cos(gt) \quad \text{and} \quad A_2(t) = e^{-\gamma t/2}\sin(gt). \tag{12}$$

Equations (10) and (11) are the basic equations that will be used to study the properties of fluorescent and intracavity photon statistics.

III. CORRELATIONS OF THE FLUORESCENT LIGHT

We now study the mean intensity (exciton number) and the spectrum of the fluorescent light. We note that the scattered field at time t and distance r in the radiation zone is proportional to the exciton operator at the retarded time $\hat{b}(t - r/c)$. Thus the fluorescent light correlations provide information about the exciton correlation function.

A. Amplitude correlation and intensity

To study the mean intensity and spectrum of fluorescent light, we calculate the two-time exciton correlation function $\langle \hat{b}^\dagger(t)\hat{b}(t+\tau)\rangle$ by using Eq. (11) and its complex conjugate,

$$\langle \hat{b}^\dagger(t)\hat{b}(t+\tau)\rangle = \left\langle \left[A_1^*(t)\hat{b}^\dagger(0) - A_2^*(t)\hat{a}^\dagger(0) + \int_0^t A_1^*(t-t')\hat{F}_e^\dagger(t')dt' - \int_0^t A_2^*(t-t')\hat{F}_c^\dagger(t')dt' \right] \times \left[A_1(t+\tau)\hat{b}(0) - A_2(t+\tau)\hat{a}(0) + \int_0^{t+\tau} A_1(t+\tau-t'')\hat{F}_e(t'')dt'' - \int_0^{t+\tau} A_2(t+\tau-t'')\hat{F}_c(t'')dt'' \right] \right\rangle. \tag{13}$$

We recall that the field and the exciton modes at the initial time are uncorrelated with the reservoirs at a later time and the reservoir noise operators are uncorrelated so that

$$\langle \hat{a}(0)\hat{F}_c(t)\rangle = \langle \hat{a}(0)\rangle\langle \hat{F}_c(t)\rangle,$$

$$\langle \hat{b}(0)\hat{F}_e(t)\rangle = \langle \hat{b}(0)\rangle\langle \hat{F}_e(t)\rangle,$$

$$\langle \hat{F}_e(t')\hat{F}_c(t)\rangle = \langle \hat{F}_e(t')\rangle\langle \hat{F}_c(t)\rangle, \tag{14}$$

where we have used the fact that the noise operators have zero mean $[\langle \hat{F}_c(t)\rangle = 0 = \langle \hat{F}_e(t)\rangle]$. Assuming that initially the exciton mode is in a number state $|n_e\rangle$ and the cavity mode is in a state $|\phi\rangle$ $(=\Sigma C_n|n\rangle$, where $|n\rangle$ is a number state), we can write the state of the exciton-photon coupled system at the initial time as $|\Psi(0)\rangle = |n_e,\phi\rangle$. Then using two-time noise correlations given in Eqs. (4)–(6), we find that the field amplitude correlation function given in Eq. (13) leads to

$$\langle \hat{b}^\dagger(t)\hat{b}(t+\tau)\rangle = \frac{e^{-\gamma\tau/2}}{2(\gamma^2+4g^2)}[\{2\gamma^2 N_e + 4g^2(N_e+N_c)\}\cos(g\tau) - 2\gamma g(N_e-N_c)\sin(g\tau) + e^{-\gamma t}\{2(\gamma^2+4g^2) \times [\bar{n}_e\cos(gt)\cos(g(t+\tau)) + \bar{n}\sin(gt)\sin(g(t+\tau))] - [(N_e+N_c)(\gamma^2+4g^2)\cos(g\tau) + \gamma^2(N_e-N_c) \times \cos(g(2t+\tau)) - 2\gamma g(N_e-N_c)\sin(g(2t+\tau))]\}], \tag{15}$$

where $\bar{n}_e$ and $\bar{n}$ are the initial mean exciton and photon numbers, respectively. From Eq. (15) we obtain the mean exciton number to be

$$\langle \hat{b}^\dagger(t)\hat{b}(t)\rangle = \frac{1}{2(\gamma^2+4g^2)}(\{2\gamma^2 N_e + 4g^2(N_e+N_c)\} + e^{-\gamma t}\{2(\gamma^2+4g^2)[\bar{n}_e\cos^2(gt) + \bar{n}\sin^2(gt)] - [(N_e+N_c)(\gamma^2+4g^2) + \gamma^2(N_e-N_c)\cos(2gt) - 2\gamma g(N_e-N_c)\sin(2gt)]\}). \tag{16}$$

Since the fluorescent intensity is proportional to the mean exciton number $\langle \hat{b}^\dagger(t)\hat{b}(t)\rangle$, in what follows we will refer to $\langle \hat{b}^\dagger(t)\hat{b}(t)\rangle$ as the fluorescent intensity.

Equations (15) and (16) show that the two-time exciton correlation function and the mean intensity of the fluorescent light depend only on the reservoir mean photon number N_c but not on the phase parameter M_c. This means that if squeezed vacuum is replaced by a thermal reservoir at a finite temperature, the photon number and spectrum of the fluorescent light will have the same behavior as described by Eqs. (15) and (16), with N_c being interpreted as the mean number of thermal quanta in the reservoir.

In the limit $t\to\infty$, we obtain the steady-state value of the two-time exciton correlation function,

$$\langle \hat{b}^\dagger(t)\hat{b}(t+\tau)\rangle_{ss} = \frac{e^{-\gamma\tau/2}}{(\gamma^2+4g^2)}[\{\gamma^2 N_e + 2g^2(N_e+N_c)\}\cos(g\tau) - \gamma g(N_e-N_c)\sin(g\tau)], \tag{17}$$

and the fluorescent intensity

$$\langle \hat{b}^\dagger(t)\hat{b}(t)\rangle_{ss} = \frac{1}{(\gamma^2+4g^2)}[\gamma^2 N_e + 2g^2(N_e+N_c)]. \tag{18}$$

At low temperatures, for which the number of the thermal phonons is negligible ($N_e=0$), Eq. (16) leads to

$$\langle \hat{b}^\dagger(t)\hat{b}(t)\rangle = \frac{1}{(\gamma^2+4g^2)}(2g^2 N_c + e^{-\gamma t}\{(\gamma^2+4g^2) \times [\bar{n}_e \cos^2(gt) + \bar{n}\sin^2(gt)] - N_c[2g^2+\gamma^2\sin^2(gt) + 2\gamma g \sin(gt)\cos(gt)]\}). \tag{19}$$

Figure 2 shows the intensity as a function of time as predicted by Eq. (19) for initially one exciton in the microcavity ($\bar{n}_e=1$). Figure 2(a) shows the dependence of fluorescent intensity on the initial mean photon number in the cavity when squeezed vacuum is absent ($N_c=0$). In this case, Eq. (19) reduces to $\langle \hat{b}^\dagger(t)\hat{b}(t)\rangle = e^{-\gamma t}[\cos^2(gt)+\bar{n}\sin^2(gt)]$. In all three cases $\bar{n}=0$, 0.5, and 2, we observe oscillations in the mean photon number at frequency g. These oscillations are due to an exchange of energy between the cavity and exciton modes. The amplitude of the oscillations depends on the mean photon number of the cavity mode at the initial time and it decreases with time due to cavity damping. An interesting behavior of the mean photon number is obtained when the initial mean photon $\bar{n}=1$. In this case, oscillations completely disappear and the mean fluorescent intensity shows pure exponential decay [$\langle \hat{b}^\dagger(t)\hat{b}(t)\rangle = e^{-\gamma t}$]. This is because in the absence of dissipation, [$\hat{a}^\dagger(t)\hat{a}(t)+\hat{b}^\dagger(t)\hat{b}(t)$] is a constant of motion for zero detuning. Then whenever the initial mean numbers of excitons and photons are equal ($\bar{n}_e = \bar{n}$), we have $\langle \hat{b}^\dagger(t)\hat{b}(t)\rangle = \langle \hat{a}^\dagger(t)\hat{a}(t)\rangle$ and therefore $\langle \hat{b}^\dagger(t)\hat{b}(t)\rangle$ must be a constant. Inclusion of damping then causes $\langle \hat{b}^\dagger(t)\hat{b}(t)\rangle$ to decay exponentially. For $\bar{n}<1$, the intensity always lies below this curve and for $\bar{n}>1$, intensity always lies above this curve. Thus this curve limits the maximum (for $\bar{n}<1$) and minimum (for $\bar{n}>1$) values of the intensity for cases with $\bar{n}\neq 1$.

The intensity of the transmitted light from a single GaAs quantum well embedded in a distributed Bragg reflector microcavity has been measured by Jacobson *et al.* [13] when the cavity is initially in vacuum state and a single exciton is in the quantum well. This experimental measurement is in excellent agreement with the theoretical predictions based on the coupled harmonic-oscillator model for the exciton-photon system. Our results for the fluorescent intensity show a qualitatively similar behavior to that of the transmitted intensity.

Figure 2(b) shows the dependence of fluorescent intensity on the squeezing parameter r when there are no photons inside the cavity initially and $\bar{n}_e=1$. For short time intervals

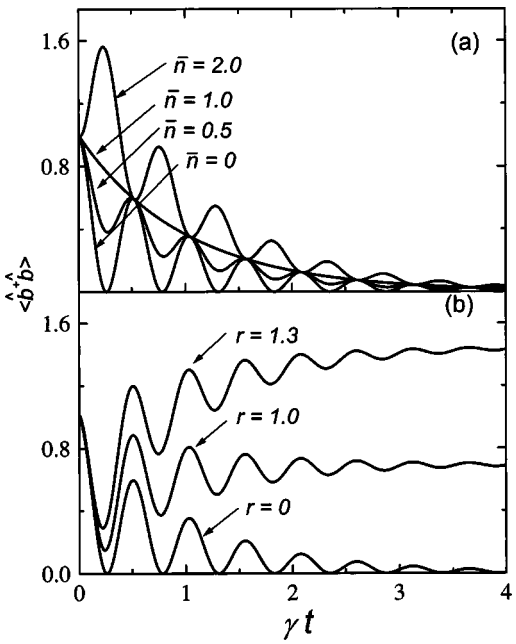

FIG. 2. Intensity of the fluorescent light as a function of scaled time γt for $g/\gamma=6.5$. (a) is for different initial mean cavity photon number $\bar{n}$ and $N_c=0$, and (b) is for different values of the squeezing parameter r and $\bar{n}=0$.

($t<\pi/g$), the effect of the squeezed vacuum on the intensity is negligible. As time increases, the squeezed vacuum effectively increases the mean fluorescence intensity in an oscillatory manner. In the steady state, the intensity approaches a value proportional to the mean photon number of the squeezed vacuum.

B. Spectrum

The spectrum of the fluorescent light in the steady state is given by

$$S(\omega) = \frac{1}{\pi}\,\mathrm{Re}\left[\int_0^\infty \exp[i\omega\tau] \times \langle \hat{b}^\dagger(t)\hat{b}(t+\tau)\rangle_{ss} d\tau\right] \Big/ \langle \hat{b}^\dagger(t)\hat{b}(t)\rangle_{ss}. \tag{20}$$

Substituting the result of Eqs. (17) and (18) in Eq. (20), we obtain the spectrum for the fluorescent light to be

$$S(\omega) = \frac{2\gamma}{\pi}\left[\frac{(\gamma^2+4g^2+4\omega^2)+\mathcal{F}(\gamma^2+4g^2-4\omega^2)}{(\gamma^2+4g^2-4\omega^2)^2+16\gamma^2\omega^2}\right], \tag{21}$$

where

$$\mathcal{F} = \frac{2g^2(N_c-N_e)}{\gamma^2 N_e + 2g^2(N_c+N_e)}. \tag{22}$$

Note that the frequency ω here should be interpreted as $\omega - \omega_c$. Because of the normalization in Eq. (20), the area

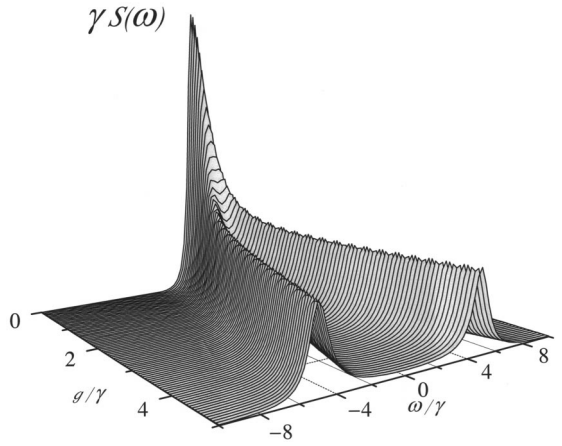

FIG. 3. Spectrum of the fluorescent light as a function of coupling strength g/γ and frequency ω/γ for $N_e=0$.

under the curve for the spectrum is 1. The spectrum given by Eq. (21) is independent of the phase parameter M_c. This indicates again that replacing squeezed vacuum by a thermal reservoir will not affect the form of the spectrum.

At low temperatures, one can neglect the number of thermal phonons ($N_e \approx 0$). In this limit, the spectrum of the fluorescent light in the steady state takes a simpler form and is independent of N_c as well,

$$S(\omega)=\frac{1}{\pi}\frac{4\gamma(\gamma^2+4g^2)}{(\gamma^2+4g^2-4\omega^2)^2+16\gamma^2\omega^2}. \tag{23}$$

Figure 3 shows a three-dimensional plot of the spectrum for $N_e=0$. In the weak-coupling limit ($g/\gamma \ll 1$), there is only a single peak at zero resonance frequency. In the strong-coupling limit ($g/\gamma \gg 1$), the spectrum shows two peaks located symmetrically at $\omega=\pm g$ about $\omega=0$. Both peaks have the same width, which depends on the exciton and photon decay rates and the strength of the coupling between them. For strong coupling, the full width at half maxima is $\Delta\omega \simeq \gamma\sqrt{1+2(\gamma/4g)^2}$. The two-peak structure in the spectrum can be explained in terms of the dressed-state picture of the exciton-field system. Energy levels in different submanifolds of the dressed states picture for the exciton-field system are equally spaced [17]. Thus several of the transitions from one submanifold to the adjacent submanifold are degenerate, resulting in only two peaks in the spectrum. Recall that the dressed levels for the atom-field system in different submanifolds are not equally spaced. In that case, an increase in excitation shows additional peaks in the emission spectrum.

We find that in the weak-field limit, the spectrum broadens as N_e increases. This is because with an increase in N_e, thermal dissipation of excitons increases. In the strong-field limit, on the other hand, the peaks are off resonance ($\omega \neq \omega_e$) and the effect of an increase of N_e on the spectrum is negligible.

C. Second-order intensity correlation function

The second-order intensity correlation function is the probability of detecting a photon at time $t+\tau$ given that one photon was detected at time t. For the fluorescent light, in the steady state, it is given by

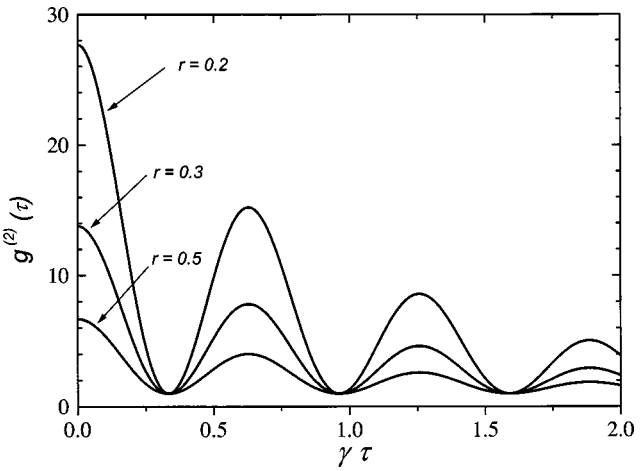

FIG. 4. Second-order intensity correlation $g^{(2)}(\tau)$ of the fluorescent light as a function of $\gamma\tau$ with $g/\gamma=5$ for different values of the squeezing parameter r. $g^{(2)}(0)\geqslant 1$ indicates bunching of photons.

$$g^{(2)}(\tau)=\frac{\langle \hat{b}^\dagger(t)\hat{b}^\dagger(t+\tau)\hat{b}(t+\tau)\hat{b}(t)\rangle_{ss}}{\langle \hat{b}^\dagger(t)\hat{b}(t)\rangle_{ss}^2}. \tag{24}$$

Using the steady-state solution,

$$\hat{b}(t)_{ss}=\int_{-\infty}^{t} e^{-(\gamma/2)(t-t')}[\cos(g(t-t'))\ \hat{F}_e(t') - \sin(g(t-t'))\hat{F}_c(t')]dt', \tag{25}$$

in Eq. (24), and the Gaussian property of the noise terms

$$\langle \hat{F}^\dagger(t_1)\hat{F}^\dagger(t_2)\hat{F}(t_3)\hat{F}(t_4)\rangle = \langle \hat{F}^\dagger(t_1)\hat{F}^\dagger(t_2)\rangle\langle \hat{F}(t_3)\hat{F}(t_4)\rangle + \langle \hat{F}^\dagger(t_1)\hat{F}(t_3)\rangle\langle \hat{F}^\dagger(t_2)\hat{F}(t_4)\rangle + \langle \hat{F}^\dagger(t_1)\hat{F}(t_4)\rangle\langle \hat{F}^\dagger(t_2)\hat{F}(t_3)\rangle, \tag{26}$$

together with the statistical independence of the noise operators for the photon and the exciton damping, we obtain the second-order intensity correlation to be

$$g^{(2)}(\tau)=1+\frac{e^{-\gamma\tau}}{[N_e(\gamma^2+2g^2)+2g^2N_c]^2} \times (|M_c|^2[2g^2\cos(g\tau)+\gamma g\sin(g\tau)]^2 + \{N_e[(\gamma^2+2g^2)\cos(g\tau)-\gamma g\sin(g\tau)] + N_c[2g^2\cos(g\tau)+\gamma g\sin(g\tau)]\}^2). \tag{27}$$

This function is shown in Fig. 4, where we have plotted its form at low temperatures where the thermal phonon number is negligible ($N_e \simeq 0$) for several values of the squeezing parameter r. In all cases, we find oscillations at frequency equal to the photon-exciton coupling constant g. We note that $g^{(2)}(0)$ is always greater than 1, indicating that the fluorescent light is always bunched [21]. This can be explained by

recalling the effect of the squeezed vacuum photons on the number of excitons. Squeezed photons entering the cavity can excite the exciton mode to a higher occupation number. Thus even if the quantum well starts from a single exciton state initially, the probability of two or more excitons is not zero. This allows emission of more than one photon simultaneously resulting in bunching. This situation is different from that of a single two-level atom in a cavity, where the atom cannot emit two photons simultaneously causing $g^{(2)}(0)$ to vanish exhibiting antibunching in the fluorescent light [21].

The effect of squeezed vacuum in the second-order intensity correlation is reflected in the amplitude of the oscillations. At low squeezing, $g^{(2)}(\tau)$ oscillates with a large amplitude which becomes smaller as we increase the degree of squeezing. Note that unlike the intensity, $g^{(2)}(\tau)$ depends on parameter M_c related to the phase correlations of the squeezed reservoir. The second term in Eq. (27) depends on the ratio $M_c/N_c[=\coth(r)]$, which becomes very large for small squeezing parameter r and decreases with an increase in r. Thus the contribution of phase correlations to $g^{(2)}(\tau)$ is much stronger for smaller values of r, resulting in a larger amplitude of oscillations.

IV. THE *Q* FUNCTION AND INTRACAVITY PHOTON NUMBER DISTRIBUTION

In Sec. II, we have derived time evolution of the operators describing the exciton and photon modes. Using the steady-state solution of these operators, we can derive the Q function for the exciton and photon modes and study the statistics of the intracavity field. We also look at squeezing in the fluorescent light.

A two-mode Q function is expressible in the form [22]

$$Q(\alpha,\beta)=\frac{1}{\pi^4}\int d^2\lambda \;\; d^2\eta \;\; \phi(\lambda,\eta) \times \exp(\lambda^*\alpha-\lambda\alpha^*+\eta^*\beta-\eta\beta^*), \qquad (28)$$

where λ and η are complex parameters and α and β are complex amplitudes corresponding to the operators $\hat{a}$ and $\hat{b}$. The characteristic function $\phi(\lambda,\eta)$ is defined in the Heisenberg picture as

$$\phi(\lambda,\eta)=\mathrm{Tr}[\rho(0)e^{-\lambda^* a(t)}e^{-\eta* b(t)}e^{\lambda a^\dagger(t)}e^{\eta b^\dagger(t)}]. \qquad (29)$$

In the steady state, Eqs. (10) and (11) lead to

$$\hat{a}(t)=\int_{-\infty}^{t}A_1(t-t')\hat{F}_c(t')dt'+\int_{-\infty}^{t}A_2(t-t')\hat{F}_e(t')dt', \qquad (30)$$

$$\hat{b}(t)=\int_{-\infty}^{t}A_1(t-t')\hat{F}_e(t')dt'-\int_{-\infty}^{t}A_2(t-t')\hat{F}_c(t')dt'. \qquad (31)$$

Substituting $\hat{a}(t)$ and $\hat{b}(t)$ in Eq. (29), using the Baker-Hausdorff identity, and averaging over the noise operators, we obtain the steady-state characteristic function to be

$$\phi(\lambda,\eta)_{ss}=\exp\Big\{-(G_1N_c+1)\lambda\lambda^*-[(1-G_1)N_c+1]\eta\eta^*+\frac{G_1}{2}[M_c^*\lambda^2+M_c\lambda^{*2}]+\frac{(1-G_1)}{2}[M_c^*\eta^2+M_c\eta^{*2}] - \frac{\gamma}{2g}(1-G_1)[M_c\lambda^*\eta^*+M_c^*\lambda\eta-N_c(\lambda^*\eta+\lambda\eta^*)]\Big\}, \qquad (32)$$

where

$$G_1=\frac{2g^2+\gamma^2}{4g^2+\gamma^2}. \qquad (33)$$

Substituting Eq. (32) into Eq. (28), and carrying out the integration, we can express the steady-state Q function for zero phase of the squeezed vacuum ($M_c^*=M_c$) as

$$Q(\alpha,\beta)=\frac{2}{\pi^2\sqrt{G_+G_-}}\exp\Big\{-\frac{1}{4G_+}\Big[[2+(e^{2r}-1)G_+](\beta+\beta^*)^2+\frac{\gamma}{g}(e^{2r}-1)(1-G_1)(\beta+\beta^*)(\alpha+\alpha^*) +[2+(e^{2r}-1)(1-G_1)](\alpha+\alpha^*)^2\Big]+\frac{1}{4G_-}\Big[[2+(e^{-2r}-1)G_1](\beta-\beta^*)^2+\frac{\gamma}{g}(1-G_1)(e^{-2r}-1)(\beta-\beta^*) \times(\alpha-\alpha^*)+[2+(e^{-2r}-1)(1-G_1)](\alpha-\alpha^*)^2\Big]\Big\}. \qquad (34)$$

Here the constants G_+ and G_- are

$$G_{\pm}=\frac{1}{2}\left[[4+2(e^{\pm 2r}-1)(1-G_1)]+(e^{\pm 2r}-1)[2+(e^{\pm 2r}-1)(1-G_1)]G_1-\frac{\gamma^2}{4g^2}(1-G_1)^2(e^{\pm 2r}-1)^2\right]. \quad (35)$$

Equation (34) is the Q function for the coupled exciton-photon system. From this we can obtain the steady-state Q function describing the intracavity field by integrating with respect to β,

$$Q_c(\alpha)=\int d^2\beta\ Q(\alpha,\beta). \quad (36)$$

Using Eq. (34) in Eq. (36), we find

$$Q_c(\alpha)=\frac{2}{\pi\sqrt{[2+(e^{-2r}-1)G_1][2+(e^{2r}-1)G_1]}}\exp\left[\frac{2}{2+(e^{-2r}-1)G_1}\left(\frac{\alpha-\alpha^*}{2}\right)^2-\frac{2}{2+(e^{2r}-1)G_1}\left(\frac{\alpha+\alpha^*}{2}\right)^2\right]. \quad (37)$$

Similarly, we can show that the Q function for the exciton mode is given by

$$Q_e(\beta)=\frac{2}{\pi\sqrt{[2+(e^{-2r}-1)(1-G_1)][2+(e^{2r}-1)(1-G_1)]}}\exp\left[\frac{2}{2+(e^{-2r}-1)(1-G_1)}\left(\frac{\beta-\beta^*}{2}\right)^2-\frac{2}{2+(e^{2r}-1)(1-G_1)}\left(\frac{\beta+\beta^*}{2}\right)^2\right]. \quad (38)$$

Q functions described by Eqs. (36) and (37) are two-dimensional Gaussian functions. In Fig. 5, we have plotted $Q_c(\alpha)$ and $Q_e(\beta)$ as functions of the Cartesian coordinates defined by $\beta=x_1+iy_1$ and $\alpha=x_2+iy_2$ in the strong-coupling limit for several different values of the squeezing parameter r. The results reveal that the two-dimensional Gaussian distribution function for the cavity field as well as the exciton show an increasing width in the x dimension than in the y dimension as the degree of squeezing increases. This behavior is more pronounced for the cavity field than for the exciton mode. This property of the Q function is a typical signature of the existence of quadrature squeezing [22]. For zero squeezing ($r=0$), we find that the distribution function for both the cavity field and the excitons approaches that for a vacuum state which has equal width in the x and y dimensions. In the week-coupling limit, we still see a significant difference in width between the two-dimension in the case of the cavity field, however in the case of excitons this difference is small.

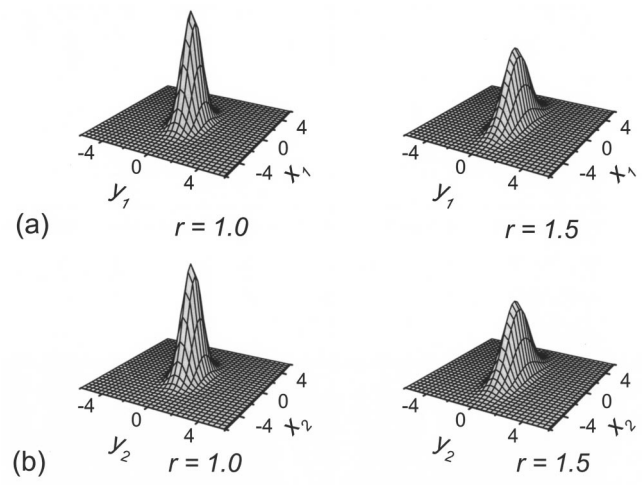

FIG. 5. Q-distribution function with $g/\gamma=5$ for different values of the squeezing parameter r, (a) for the fluorescent light and (b) for the cavity mode.

A. Quadrature squeezing

To study quadrature fluctuations, we define two Hermitian quadrature operators $\hat{b}_1=\hat{b}^\dagger+\hat{b}$ and $\hat{b}_2=i(\hat{b}^\dagger-\hat{b})$ for the exciton. Using the Q function in Eq. (38), one can evaluate the variances in these two quadratures as

$$\langle(\Delta\hat{b}_1)^2\rangle=1+\frac{2g^2}{4g^2+\gamma^2}[\exp(2r)-1],$$

$$\langle(\Delta\hat{b}_2)^2\rangle=1-\frac{2g^2}{4g^2+\gamma^2}[1-\exp(-2r)]. \quad (39)$$

Similarly one can easily show that for the cavity mode the variances in the two quadratures $\hat{a}_1=\hat{a}^\dagger+\hat{a}$ and $\hat{a}_2=i(\hat{a}^\dagger-\hat{a})$ are given by

$$\langle(\Delta\hat{a}_1)^2\rangle=1+\frac{2g^2+\gamma^2}{4g^2+\gamma^2}[\exp(2r)-1],$$

$$\langle(\Delta\hat{a}_2)^2\rangle=1-\frac{2g^2+\gamma^2}{4g^2+\gamma^2}[1-\exp(-2r)]. \quad (40)$$

Equations (39) and (40) describe quantum fluctuations in the two quadratures of the excitons and the intracavity field.

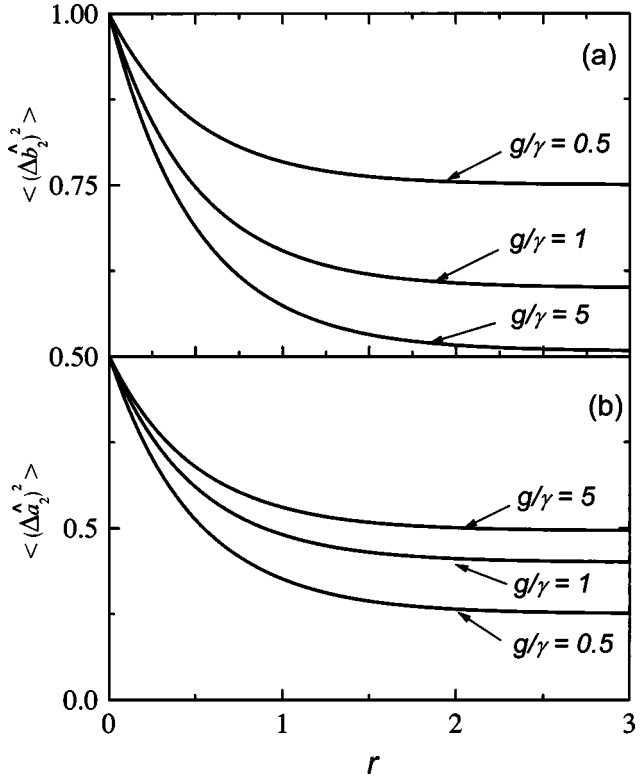

FIG. 6. Variance of the squeezed quadrature as a function of the injected field squeezing parameter r for different coupling strength g/γ for (a) the fluorescent light and (b) the cavity mode.

We note that $\langle(\Delta\hat{b}_1)^2\rangle$, $\langle(\Delta\hat{a}_1)^2\rangle>1$ and $\langle(\Delta\hat{b}_2)^2\rangle$, $\langle(\Delta\hat{a}_2)^2\rangle<1$ for nonzero r and $g>0$. Quadrature variance below 1 indicates quadrature squeezing. The amount of squeezing in each mode depends on the strength of coupling between the exciton and cavity field as well as the degree of squeezing of the injected light. We have illustrated this in Figs. 6 and 7, where we plot the variance in the second quadrature as a function of r and g. Figure 6(a) shows that the degree of squeezing in the exciton mode and therefore in the fluorescent light increases with increased coupling between the exciton and cavity modes. For the cavity field [Fig. 6(b)], on the other hand, although the amount of squeezing increases with increasing r, the maximum achievable noise reduction decreases as the coupling with the exciton mode increases.

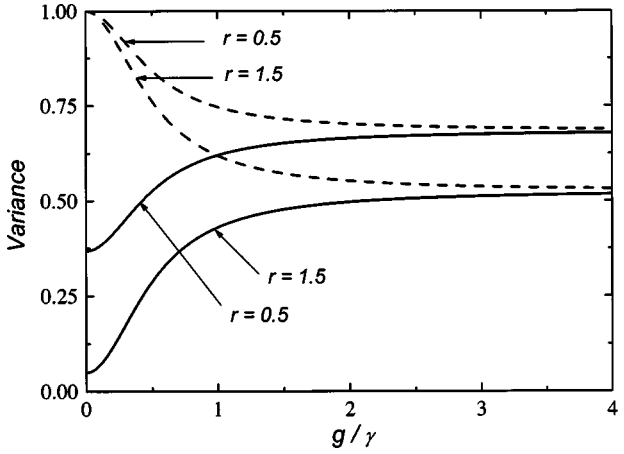

FIG. 7. Variance of the squeezed field quadratures of the cavity mode (solid curves) and the fluorescent light (dash curves) as a function of coupling strength g/γ for different squeezing parameter r.

In Fig. 7, we plot quadrature variances as functions of coupling constant g. For zero coupling, the exciton mode does not show any squeezing as there is no interaction between the exciton and the cavity mode. However, since the cavity is coupled to squeezed vacuum, we see squeezing in the cavity mode. We observe that in the strong-coupling ($g \gg \gamma$) and large squeezing parameter ($r \gg 1$) limit, both variances approach $\frac{1}{2}$. Thus fluorescent light gains a 50% noise reduction below the vacuum level while the cavity field loses squeezing and approaches a 50% noise reduction.

B. Photon number distribution

Next we consider the probability $P(n)$ that the cavity has n photons in the steady state. This probability in terms of the Q function is expressible as [23,24]

$$P(n)=\frac{\pi}{n!}\frac{\partial^{2n}}{\partial\alpha^n\partial\alpha^{*n}}[Q(\alpha,\alpha^*)e^{-\alpha\alpha^*}]|_{\alpha=\alpha^*=0}. \quad (41)$$

Using the Q function of Eq. (37) and on performing the necessary differentiation, we obtain

$$P(n)=\frac{1}{\sqrt{[2+(e^{-2r}-1)G_1][2+(e^{2r}-1)G_1]}}\left[1-\frac{4+(e^r-e^{-r})^2G_1}{[2+(e^{-2r}-1)G_1][2+(e^{2r}-1)G_1]}\right]^n \times\sum_{k=0}^{[n]}\frac{n!}{2^{2k-1}k!^2(n-2k)!}\left[\frac{(e^r+e^{-r})}{(e^r-e^{-r})[1-G_1]}\right]^{2k}, \quad (42)$$

where

$$[n]=\begin{cases} n/2 & (\text{for even } n),\\ (n-1)/2 & (\text{for odd } n). \end{cases} \quad (43)$$

With the help of this distribution or the Q function in Eq. (38), it can be shown that the mean intracavity photon number is $\bar{n}_c = G_1 N_c$. In terms of the mean photon number, the photon number distribution is expressible as

$$P(n) = \frac{N_c[\bar{n}_c(1+\bar{n}_c)N_c^2 - (\bar{n}_c|M_c|)^2]^n}{[(1+\bar{n}_c)^2 N_c^2 - (\bar{n}_c|M_c|)^2]^{n+1/2}} \sum_{k=0}^{[n]} \frac{n!}{2^{2k}k!^2(n-2k)!}\left[\frac{|M_c|N_c}{(1+\bar{n}_c)N_c^2 - \bar{n}_c|M_c|^2}\right]^{2k}, \tag{44}$$

where N_c and M_c defined in Eq. (5) are related to squeezing parameter r. The intracavity photon number distribution $P(n)$ depends on the mean photon number of the intracavity field as well as the amount of squeezing in the injected field. If thermal light is injected instead of squeezed light, we have $|M_c| = 0$ and the photon number distribution reduces, as expected, to

$$P(n) = \frac{[\bar{n}_c]^n}{[1+\bar{n}_c]^{n+1}}. \tag{45}$$

The distribution $P(n)$ is shown in Figs. 8(a) and 8(b) in the weak- and strong-coupling limits, respectively. In the weak-coupling limit, $\bar{n}_c = [(2g^2+\gamma^2)/(4g^2+\gamma^2)]N_c \simeq N_c$, as one can see from Fig. 8(a), the photon number distribution shows even-odd oscillations with higher probability for an even number of photons than for an odd number of photons. In the strong-coupling limit, the intracavity mean photon number $\bar{n}_c \simeq 0.5 N_c$. For this case, we see [Fig. 8(b)] that even-odd oscillations are damped out and $P(n)$ exhibits long tails as the squeezing parameter r increases. Increasing r results in large values of squeezed vacuum mean photon number that lead to large cavity mean photon number. The long tails in the photon number distribution are due to the large intensity fluctuation of the injected squeezed vacuum, which grows exponentially with increasing squeezing parameter r [9,25].

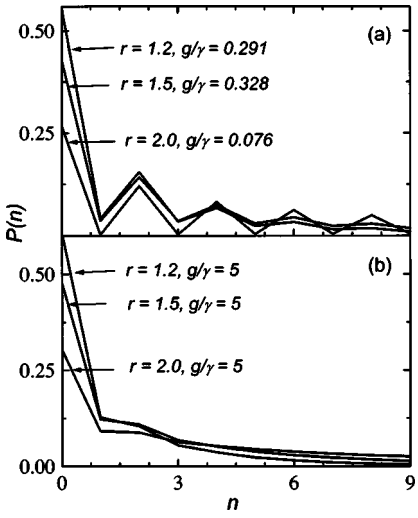

FIG. 8. Photon number distribution for the cavity mode for different values of r in (a) the weak-coupling limit and (b) the strong-coupling limit.

V. CONCLUSION

In conclusion, we have studied the quantum statistical properties of the light emitted by a quantum well in a microcavity when the cavity is injected with squeezed vacuum. We have solved the quantum Langevin equations for the coupled field-exciton modes and constructed the associated Q-distribution function. Using these equations, we have studied the intensity, field spectrum, second-order intensity correlation, and field quadrature fluctuations for the fluorescent light. We have also studied quadrature fluctuations and photon number distribution for the intracavity field.

We find that the intensity of the fluorescent light from a quantum well exhibits oscillations and the frequency of oscillation depends on the strength of coupling between the cavity and exciton modes. The amplitude of the oscillations depends on the initial cavity mean photon number as well as the mean photon number of the injected squeezed vacuum. The intensity shows an interesting feature when the initial mean cavity photon number is equal to the mean number of excitons and squeezed vacuum is turned off. Under these conditions, the oscillations in the intensity of the fluorescent light are completely washed out and the fluorescent intensity exhibits pure exponential decay. On the other hand, in the presence of the squeezed vacuum the intensity always shows oscillations and the amplitude of the oscillations reaches a steady-state value that is proportional to the strength of the squeezed vacuum. The spectrum of the fluorescent light shows normal mode splitting in the strong-coupling limit and the linewidths of the two normal modes for $\gamma \ll 2g$ are equal to the common damping rate of the field and exciton.

The second-order intensity correlation function $g^{(2)}(0)$ is always greater than 1, indicating that the fluorescent light is always bunched [21]. This is because an exciton mode, unlike a two-level atom, can emit two or more photons simultaneously. The second-order intensity correlation also shows oscillations at frequency equal to the coupling strength g. Thus these oscillations provide a measure of coupling strength between the cavity and exciton modes. The amplitude of these oscillations is larger for lower squeezing than that for higher squeezing.

We have found that the Q functions for the exciton and the cavity modes are two-dimensional Gaussian functions with a narrower width in one dimension than in the other. This indicates the field quadratures for the cavity mode as well as for the fluorescent light are squeezed. The results for the quadrature fluctuations reveal that if the cavity is injected with a perfectly squeezed light, a 50% noise reduction below the vacuum level can be achieved in the fluorescent light and

the cavity mode in the strong-coupling limit. Using the Q function, we have also calculated the steady-state intracavity photon number distribution and the results have shown that $P(n)$ exhibits a long tail for highly squeezed light due to large intensity fluctuations. In the weak-coupling limits, the photon number distribution shows even-odd oscillations.

ACKNOWLEDGMENTS

This work was supported in part by the Office of Naval Research and Arkansas Science and Technology Authority. D.E. acknowledges support from the ICSC World Laboratory.

[1] J. J. Hopfield, Phys. Rev. **112**, 1555 (1958).
[2] C. Weisbuch, M. Nishioka, A. Ishikawa, and Y. Arakawa, Phys. Rev. Lett. **69**, 3314 (1992).
[3] E. T. Jaynes and F. W. Cummings, Proc. IEEE **51**, 89 (1963).
[4] M. G. Raizen, R. J. Thompson, R. J. Brecha, H. J. Kimble, and H. J. Carmichael, Phys. Rev. Lett. **63**, 240 (1989).
[5] R. J. Thompson, G. Rempe, and H. J. Kimble, Phys. Rev. Lett. **68**, 1132 (1992).
[6] Y. Zhu, D. J. Gauthier, S. E. Morin, Q. Wu, H. J. Carmichael, and T. W. Mossberg, Phys. Rev. Lett. **64**, 2499 (1990).
[7] C. Wang and R. Vyas, Phys. Rev. A **51**, 2516 (1995); *ibid.* **55**, 823 (1997).
[8] C. Wang and R. Vyas, Phys. Rev. A **54**, 4453 (1996).
[9] D. Erenso and R. Vyas, Phys. Rev. A **65**, 063808 (2002).
[10] Y. Yamamoto, F. Matinaga, S. Machida, A. Karlsson, J. Jacobson, G. Björk, and T. Mukai, J. Phys. II **3**, 39 (1993).
[11] R. Houdré, R. P. Stanley, U. Oesterle, M. Ilegems, and C. Weisbuch, J. Phys. IV **3**, 51 (1993); Phys. Rev. B **49**, 16 761 (1994).
[12] H. Cao, J. Jacobson, G. Björk, S. Pau, and Y. Yamamoto, Appl. Phys. Lett. **66**, 1107 (1995).
[13] J. Jacobson, S. Pau, H. Cao, G. Björk, and Y. Yamamoto, Phys. Rev. A **51**, 2542 (1995).
[14] T. B. Norris, J. K. Rhee, C. Y. Sung, Y. Arakawa, M. Nishioka, and C. Weisbuch, Phys. Rev. B **50**, 14 663 (1994).
[15] S. Pau, G. Björk, J. Jacobson, H. Cao, and Y. Yamamoto, Phys. Rev. B **51**, 14 437 (1995).
[16] H. Wang, Y. Chough, S. E. Palmer, and H. J. Carmichael, Opt. Express **1**, 370 (1997).
[17] Y. Yamamoto, F. Tassone, and H. Cao, *Semiconductor Cavity Quantum Electrodynamics* (Springer-Verlag, Berlin, 2000).
[18] E. Hanamura, J. Phys. Soc. Jpn. **29**, 50 (1970).
[19] F. Bassani, F. Ruggiero, and A. Quattropani, Nuovo Cimento Soc. Ital. Fis., D **7**, 700 (1986).
[20] C. W. Gardiner and M. J. Collett, Phys. Rev. A **31**, 3761 (1985).
[21] R. Vyas and S. Singh, J. Opt. Soc. Am. B **17**, 634 (2000).
[22] D. F. Walls and G. J. Milburn, *Quantum Optics* (Springer-Verlag, Berlin, 1994).
[23] J. Anwar and M. S. Zubairy, Phys. Rev. A **45**, 1804 (1992).
[24] B. Daniel and K. Fesseha, Opt. Commun. **151**, 384 (1998).
[25] H. P. Yuen, Phys. Rev. A **13**, 2226 (1976).